AFM-Based Single Molecule Force Spectroscopy of End-Grafted Poly(acrylic acid) Monolayers

Lars Sonnenberg,[†] Julien Parvole,[‡] Oleg Borisov,[‡] Laurent Billon,[‡] Hermann E. Gaub,*[,†] and Markus Seitz[†]

Lehrstuhl für Angewandte Physik & Center for NanoScience, Ludwig-Maximilians-Universität, Amalienstr. 54, 80799 München, Germany, and Laboratoire de Physico-Chimie des Polymères, Université de Pau et des pays de l'Adour, Hélioparc Pau-Pyrénées, 2 Av Président Angot, 64053 Pau Cedex 09, France

Received March 21, 2005; Revised Manuscript Received November 2, 2005

ABSTRACT: AFM-based single molecule force spectroscopy has been applied to study the detachment of poly(acrylic acid) (PAA) chains preadsorbed onto a silicon nitride tip surface at varied pH. In particular, monolayers of end-grafted chains prepared by nitroxide-mediated polymerization initiated from silica substrates were brought into close contact with the silicon nitride tip of an AFM. The detachment of PAA chains from the tip surface is reflected by a set of constant-force plateaus in the AFM force spectra. From those, comprehensive information about the molecular length distribution of surface-grafted polymers, about their conformation, and about their interaction with the tip as a function of pH is deduced. At neutral pH, the plateau-length distribution well reproduces the molecular weight distribution of the grafted polymers as obtained by GPC. At high pH, increasing electrostatic repulsion between PAA and the tip surface reduces the strength of adsorption, which is manifested in a decrease of average plateau lengths and measured detachment forces. At low pH, complex force spectra and a bimodal distribution of apparent molecular lengths are obtained, reflecting the poor solubility of protonated PAA chains in water as well as polymer−substrate interactions.

Introduction

Polymers anchored to solid interfaces are in the focus of materials science, as they offer a broad range of applications, from tribology to biomedicine, where specific properties of the interfaces are tuned by proper surface modification. In general, water-based systems offer the best opportunity to combine a multitude of independently tunable interactions, in particular, hydrophobic and electrostatic ones. Hereby, polyelectrolytes are of particular importance, as their electrostatic interactions can be affected, and thus tuned, by ionic strength as well as by pH (in the case of pH-sensitive polyelectrolytes and surfaces).

For the creation of end-grafted polymer layers on solid substrates, one most prominent method is the so-called "grafting-from" technique. Because of its proficiency to lead to macromolecules with well-defined architecture and macromolecular dimensions, controlled/living radical polymerization (CRP) and in particular nitroxide-mediated polymerization (NMP) has been extensively described for almost 10 years.[1−8] Hereby, post-modification and/or copolymerization enable to create grafted amphiphilic (co)polymer layers with controlled hydrophilic/hydrophobic balance, ionic groups, gradient of properties along the chemical sequence, etc. This opens a large perspective for the design of polymeric monolayers with predetermined and responsive features adjustable for different applications.

For a better understanding of the structure−property relationships in these polymer layers, which is necessary for the tuning of the materials' properties, there is need for characterization at the molecular level. Several techniques, such as SFA and AFM, have been employed to study the conformation of surface-attached polymers in ensemble measurements. The interpretation of these experiments was based on well-established theories for end-grafted polymers and polyelectrolytes.

Among the experimental methods for the studying of conformations and interactions of macromolecules, AFM-based force spectroscopy is one of the most powerful and sensitive ones. At the level of individual polymer chains, it has been successfully used to measure intra- and intermolecular forces with high precision.[9−12] The method enables to elucidate collective effects arising from confinements and interactions between substrate-grafted chains subjected to extensional deformation,[13] and it was proved useful in the investigation of polymer conformations and molecular bond strengths at the single molecule level.[9,14−16]

Finally, and most importantly for the context of this work, the interactions of individual macromolecules with solid−liquid interfaces have been successfully studied by AFM force spectroscopy.[17] The loop-size distribution of adsorbed polymer chains at the solid substrate[18] and the forces, which are necessary to pull them off the substrate,[18−20] were measured. For polyelectrolytes on oppositely charged substrates, it was found that the magnitude of these desorption forces depends linearly on the Debye screening length and on the linear charge density of the polyelectrolyte chains.[17,21] Further details of non-Coulomb contributions to the desorption force as well as the influence of the solvent were revealed.[22]

In a paper by Li et al.,[23] the elastic behavior of poly(acrylic acid) adsorbed on a glass substrate was studied by AFM force spectroscopy. Hereby, a distribution of "extension lengths" was given. However, as the adsorbed layer consists of an entangled network of polymer chains, this distribution rather reflects the lengths of those polymer segments in the interfacial layer, which are accessible for stretching, but not the full contour lengths of the poly(acrylic acid) chains.

[†] Ludwig-Maximilians-Universität München.
[‡] Université de Pau et des pays de l'Adour.
* Corresponding author.

10.1021/ma0505880 CCC: $33.50
Published on Web 12/08/2005

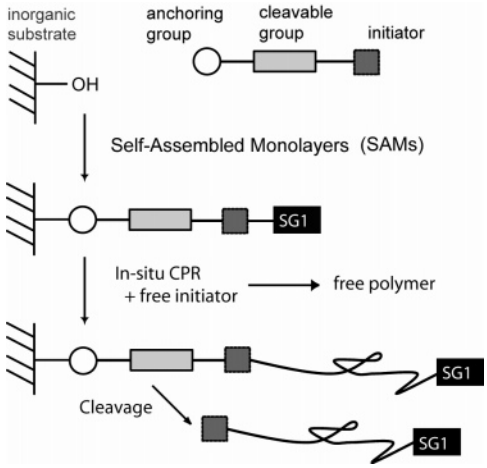

Figure 1. Concept for the synthesis of covalently attached polymer monolayers via controlled/living radical polymerization using immobilized initiators (grafting from technique).

In a paper by Walker et al.,[24] a layer of poly(dimethylsiloxane) grafted to a silica substrate was investigated by AFM in water. Again, the elastic profiles of single polymer chains were recorded, and the distribution of contour lengths of the polymer segments between the tip and the surface was given, merely reproducing the expected polymer length distributions. However, since poly(dimethylsiloxane) is not water-soluble, these measurements were performed under bad-solvent conditions, where the tethered polymers are present in a collapsed conformation.

Here, we show the applicability of AFM-based measurements for the investigation and structural characterization of pH-sensitive polyelectrolyte chains on solid substrates. In particular, we are using poly(acrylic acid) grafted from silica substrates by controlled radical polymerization, which physically interact with an AFM tip, namely adsorbing upon approaching and desorbing upon retraction of the tip from the substrate. The measurement of the interaction forces during the desorption of individual polymer chains yields the full lengths of the adhering chains as well as their adhesion forces.

Since the conformation of poly(acrylic acid) depends on the pH of the aqueous buffer, we were able to study the effect of the solvent condition on the accuracy of the determined molecular length distributions.

The scope of this paper therefore is to investigate the experimental regimes under which the correlation of length histograms from AFM experiments with the molecular structure of the grafted polymer layers is possible.

For this purpose, the AFM data will then be compared to those obtained by standard methods, namely, gel permeation chromatography (GPC) and X-ray photoelectron spectroscopy (XPS). Our results promise the implementation of the AFM method as an analytical tool for the analysis of chain length distributions and grafting densities of substrate-grafted polymer layers.

Materials and Methods

Sample Preparation and Characterization. The covalently attached polymer monolayers were synthesized via controlled/living radical polymerization using immobilized initiators. The concept is shown in Figure 1. NMP was applied for the preparation of well-defined polymer monolayers end-grafted onto silica surfaces (vinyl and acrylic monomers).[25−30] For this purpose, preformed functionalized azoic[25,26,30,31] or alkoxyamine[26−29] initiators were synthesized and covalently attached to silica substrates. The initiator used in this study consists of an azo group, which is structurally similar to AIBN, and two monochlorosilane headgroups ($SiMe_2Cl$) that connect the initiator through silanol moieties (SiOH) to the surface of the substrate. The ester group connecting the initiating group and the anchor group can act as a break-seal group under transesterification conditions. Hence, this ester can be cleaved after completion of the layer formation, and the polymer can be removed from the surface for bulk characterization.[25−31]

In the second step, radical polymerization was initiated from the surface under controlled conditions. Hereby, the acrylic monomer reacts with the surface-attached initiator. Briefly, to an initiator-grafted wafer was added a mixture of the monomer acrylic acid (AA), the initiator 2,2′-azobis(isobutyronitrile) (AIBN, ratio [AA]/2[AIBN] = 2000), and the counter radical SG1 ([SG1]/[AIBN] = 2.1). This mixture was thoroughly degassed and heated to 120 °C for chosen periods of time. After the polymerization time, the silicon wafer was continuously washed free of any adsorbed polymer (PAA) with water and 1,4-dioxane. Then, the wafer was dried and stocked under nitrogen.

In preliminary experiments, the free polymer chains were characterized with gel permeation chromatography (GPC) in THF after methylation of PAA to poly(methyl acrylate), yielding an organo-soluble polymer. GPC characterization was performed using a 2690 Waters Alliance System with THF as the eluent. It was equipped with four Styragel columns HR 0.5, 2, 4, and 6 working in series at 40 °C, a 2410 Waters refractive index detector, and a 996 Waters photodiode array detector. A calibration curve established with low-polydispersity polystyrene standards was used for the determination of the molecular weights. The GPC data indicate that the (average) contour length of the chains is ∼590 nm with a polydispersity (PD) of 1.3. At low grafting densities (<0.01 chain nm^{-2}) values of the polymer surface density cannot be measured with sufficiently high accuracy. Therefore, the X-ray photoelectron spectroscopy (XPS) data had to be compared to the data from samples with known high grafting densities.[32] Analyzing the intensities of the carbon and silicon peaks in the XPS spectra, the grafting density could be estimated as ∼0.005 chain nm^{-2}. For further details on polymerization and characterization, the reader is referred to previous publications by Billon[33] and Charleux.[34]

AFM Force Spectroscopy. The force spectroscopy experiments were conducted on a home-built AFM instrument using silicon nitride cantilevers (Microlever) purchased from Veeco Instruments. Nominal spring constants were calibrated using the thermal oscillation method[35] before the first force−extension curve was measured.

The experimental strategy adopted in the present study assumes that substrate-grafted polymers reversibly adsorb onto the AFM tip when the tip approaches the substrate surface and desorb from the AFM tip when it retracts from the substrate. The force acting on the AFM tip upon retraction was measured. The corresponding force−extension profiles exhibit a set of characteristic plateaus resembling those obtained in earlier AFM studies on polymer desorption of tip-attached polymers from bare substrates,[21,22] in which the difference in the heights of the plateaus reflects the magnitude of the desorption force of a single polymer chain (Figure 2), and the plateau length is proportional to the contour length of the adsorbed chain segments.

All AFM measurements were performed in an aqueous environment. The samples of substrate-grafted poly(acrylic acid) were investigated at varied pH in aqueous solution containing 100 mM NaCl. As we intended to focus on the pH-dependent properties of poly(acrylic acid) here, a NaCl concentration of 100 mM was used in order to reduce the force contribution of electrostatic interactions between the tip and the polymer chains. To select a set of individual polymer chains, which represent the molecular weight distribution of the substrate-grafted ensemble, data were collected at different spots on the surface and thus for different poly(acrylic acid) chains.

The tip positions were chosen randomly on a 4 × 3 mm^2 area on the surface. Typically, 100 force−extension curves were measured for each investigated pH value and for each of 10 different spots of the sample. Repeated measurements on the same spot resulted in reproducible force−distance curves, indicating that no polymer chains were worn off from the substrate. Also, before and

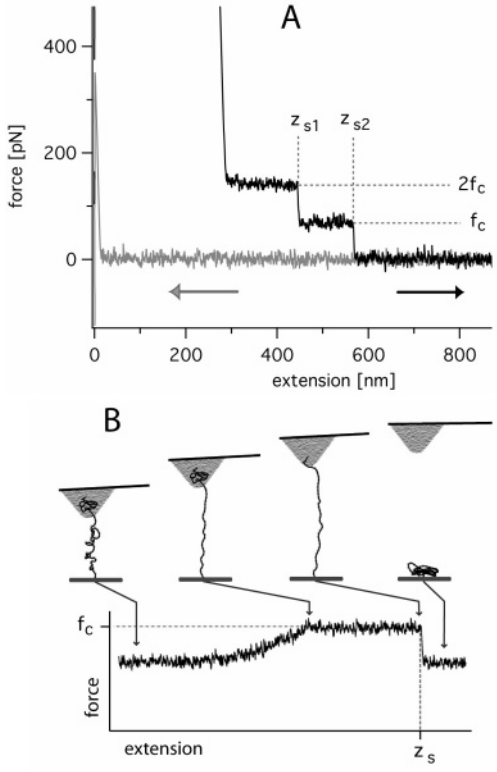

Figure 2. (A) Typical force−distance curve obtained in a single molecule desorption experiment with a surface-grafted polymer monolayer and a nonfunctionalized AFM tip. Upon contacting the tip with the substrate, surface-grafted polyelectrolyte chains are allowed to adsorb on the tip. Upon retracting the tip, typically, a strong adhesive peak is observed at small tip−substrate separation. Upon further increasing the tip−substrate distance, the continuous desorption of successive chain segments is reflected by a plateau of constant force, whereas the complete desorption of the entire polymer chain results in a sudden drop of the adhesive force. (B) In rare cases, single nonadsorbed (bridging) segments between tip and substrate may still exist, which are reflected by a nonlinear increase in the stretching force before the successive desorption of adsorbed monomers sets in.

after each set of experiments (in which different surface spots were investigated), control measurements were made, in which the interaction of the AFM tip with bare silica substrates was recorded to make sure that no polymers were transferred to the AFM tip during the course of the experiment. It was found that the tip−silica interaction profile was not altered after the experiment.

The plateaus were analyzed in respect of desorption forces and plateau lengths. The results were plotted as histograms showing the statistical distributions, i.e., the number of events observed for certain desorption forces or desorption lengths, respectively. Thereby, all histograms presented in the following constitute superpositions of measurement series at different surface positions carried out under the same conditions, representing the ensemble of the surface-grafted poly(acrylic acid) molecules.

Note that because of the "unspecific" interaction of the silicon nitride tips with the substrate, force−extension curves may show a high unspecific adsorption peak at short tip−substrate distances, which under certain conditions may extend to a few hundred nanometers. Thus, only desorption events extending beyond this range can be detected in such cases. In our measurements, most of the polymer chains exhibit sufficiently large contour lengths, so that the unspecific adsorption peak does not affect the measured length distribution. (For shorter chains, the influence of the unspecific adsorption peak would manifest itself in an artificial cutoff of the distribution at shorter chain lengths.)

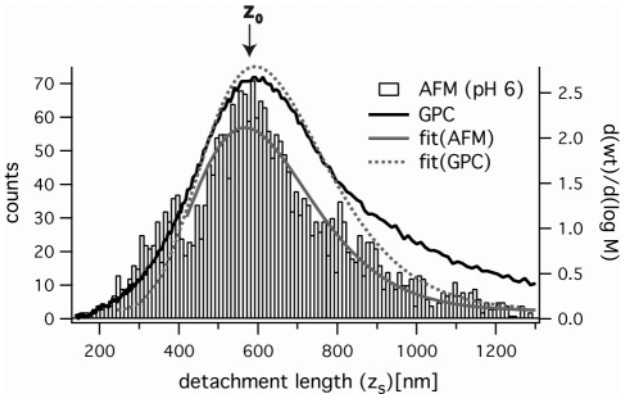

Figure 3. Molecular weight/length distributions obtained by single molecule force spectroscopy at pH 6 (histogram) and by GPC (black curve). Both data sets were fitted with a log-nor distribution with constant width (= log(PD) = 0.26), resulting in maxima positions z_0 of 572 nm (solid curve) and 592 nm (dotted curve).

Results

Distribution of Detachment Lengths at pH 6: Comparison with GPC. The comparison between AFM measurements (plateau length distribution) at pH 6 and GPC experiments is shown in Figure 3. Very narrow molecular weight distributions, e.g., instantaneous MWD, can be well characterized by Flory or Poisson distributions. A broader MWD can be described by log-nor distributions:[36]

$$P(z) = P_0 \exp[-0.5(\log(z/z_0)/t)^2]$$

The maximum of the distribution is characterized by z_0, corresponding to the number-average of the apparent polymer chain lengths within the interfacial layer. The width of the curve is given by t, which is related to the polydispersity over t = log(PD). The factor P_0 ensures normalization of the distribution. For the distributions shown in Figure 3, the fitting process determines z_0 = 592 nm for the GPC data and z_0 = 572 nm for the AFM data.

Figure 3 shows that the molecular length distributions obtained by GPC and single molecule force spectroscopy are in good agreement. Hence, single molecule force spectroscopy can be successfully applied as a tool for molecular weight determination of surface-grafted poly(acrylic acid) chains under the conditions of neutral to slightly alkaline pH. In contrast to GPC, the chains do not have to be cleaved from the substrate (cf. experimental section) but can be analyzed unaltered. In addition, unprecedented by other methods, polymer length distributions at the surface can be spatially resolved at the level of individual molecules. Further studies are required to define grafting densities and chain lengths accessible by single molecule force spectroscopy characterization.

pH Dependence of AFM-Determined Length Distribution. The distribution of the apparent polymer chain lengths of the surface-grafted poly(acrylic acid) molecules as observed in the desorption profiles depends on the pH (Figure 4). Thus, different measurement series were conducted for various pH values between pH 2.5 and 11. Figure 5 shows the experimentally obtained average apparent polymer lengths z_0 as a function of pH. While the maximum in the length distribution, z_0, remains merely constant at 570 nm for pH ≤ 7, z_0 decreases significantly between pH 8 and 11 to z_0 = 430 nm. It was further observed that the desorption forces recorded at alkaline pH were lowered by an average of ∼3 pN as compared to the desorption forces at pH ≤ 6 (i.e., the average desorption force of 73 pN at pH 6 drops to ∼70 pN at pH 10).

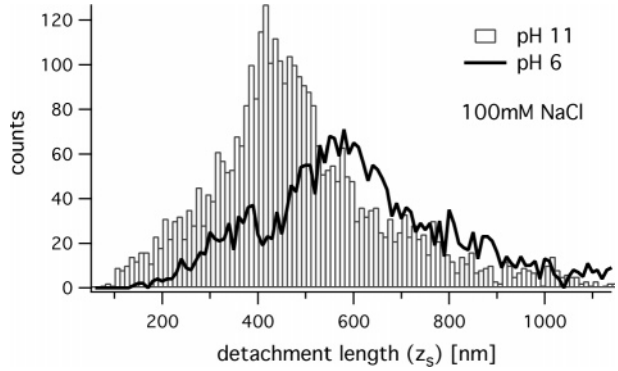

Figure 4. Molecular length distributions measured by single molecule force spectroscopy in aqueous buffer containing 100 mM NaCl at pH 6 and 11. The number of analyzed curves is identical ($N = 1000$) for both conditions. At higher pH, the maximum position of the distribution z_0 is shifted to smaller values, and the number of observed plateaus in the force−distance traces is increased.

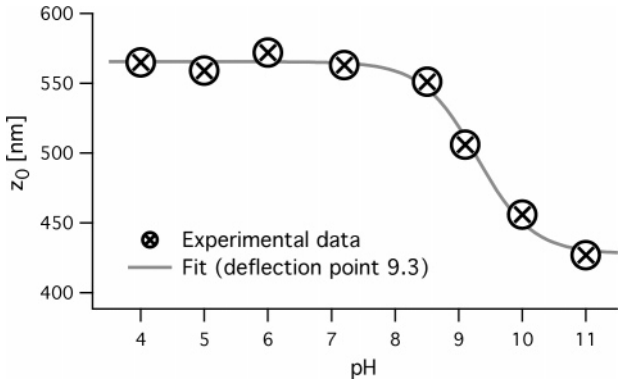

Figure 5. Plot of the maximum position z_0 taken from the experimentally obtained length histograms against the pH of the buffer solution.

The experimental data can be well fitted by the following empirical equation:

$$z_0 = c_1 - c_2 \times 10^{\mathrm{pH}-\mathrm{p}K^*}$$

Therein, z_0 is the observed average polymer length at a certain pH and c_1, c_2, and pK* are adjustable (fitting) parameters. The best fit gave $c_1 = 566$ nm, $c_2 = 140$ nm, and pK* = 9.3. However, note that pK* is a fit parameter, which does not necessarily correspond to the effective pK value of the acrylic acid chains in the grafted layer (which mainly depends on intermolecular Coulomb interactions).[37,38]

The frequency of desorption events may also be deduced from the measured desorption traces and can be given as the number of observed plateaus per curve (i.e., the number of different individual polymer chains involved in the desorption process upon retraction of the tip). This frequency was also found to depend on the pH of the buffer solution: increasing pH yields an increased number of observed plateaus per curve as seen in Figure 4 by the larger number of overall counts for the same number of analyzed desorption traces.

As the frequency of desorption events is related to the total number of chains adherent to the tip during the desorption events, one may estimate this number from the distributions: the number of chains within the contact area between tip and substrate is obtained as the integrated frequency of events divided by the number of analyzed desorption traces. For the curves shown in Figure 4, the number of analyzed traces is $N = 1000$. The average number of polymer chains, n, adherent to the tip throughout all AFM experiments on surface-grafted poly(acrylic acid) layers synthesized under the same conditions (as given in the experimental section) was calculated as approximately $n = 3$.

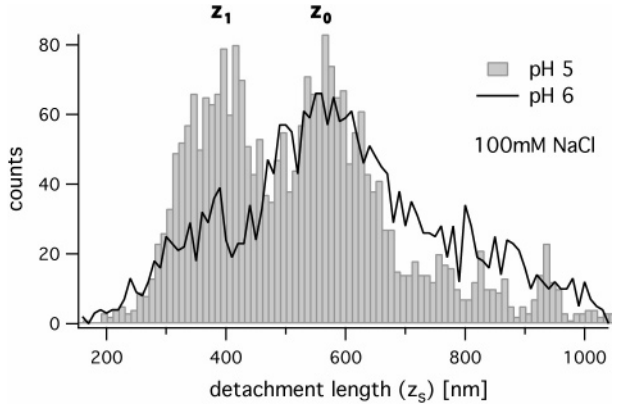

Figure 6. Molecular length distributions measured by single molecule force spectroscopy at pH 5 and 6. The number of analyzed curves is identical ($N = 1000$). At pH 5, a bimodal distribution is observed (maximum positions are noted z_1, z_0).

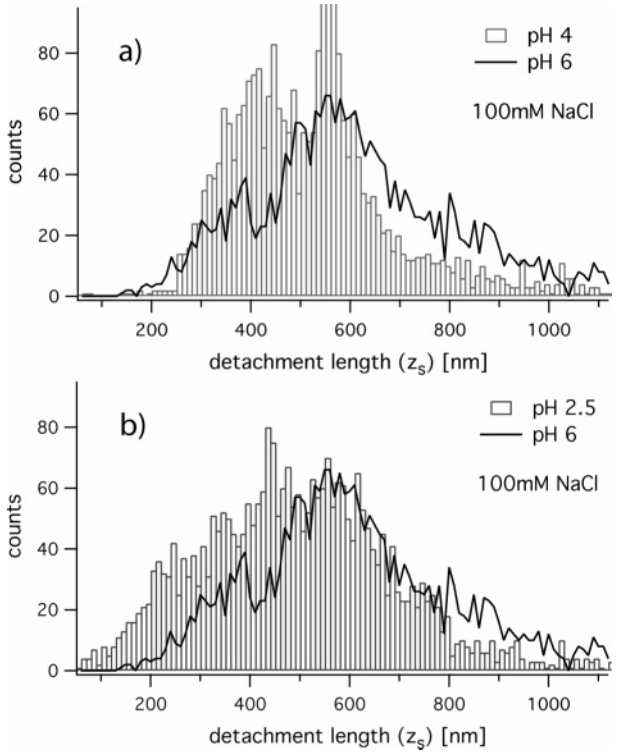

Figure 7. Molecular length histograms observed under acidic conditions: (a) pH 4; (b) pH 2.5 (each plotted in comparison to the molecular length distribution for pH 6).

Bimodal Plateau Length Distribution at pH < 6. Upon decreasing the pH from pH 6 to pH 4, the plateau length distribution becomes bimodal. That is, the histograms of the recorded plateau lengths exhibit an additional peak at shorter lengths (Figure 6), which was not considered for the above determination of the average chain lengths z_0.

While still negligible at pH 6, the second peak at lower plateau length ($z_1 \approx 400$ nm) becomes more pronounced at pH 5, where both maxima have almost the same intensity (i.e., the same frequency of events). When further decreasing the pH (Figure 7a), the lower length peak broadens but can still be distinguished from the higher length peak (which keeps its position at z_0). At pH 2.5 (Figure 7b), a broad distribution is

observed which may be viewed as a continued broadening of the lower length peak, finally merging with the higher length peak. Hereby, the frequency of events found at $z_0 = 570$ nm appears to remain merely unchanged.

Estimation of Polymer Grafting Density. The characterization of surface-grafted polymer layers in terms of grafting densities with single molecule force spectroscopy requires the knowledge of the AFM tip size and the number of grafted polymer chains under the tip area. For the microlever tips used in our experiments a tip curvature radius of 20−40 nm is reported by the distributor. It can be assumed that the area on the substrate in contact with the tip during the experiment is of approximately the same size (i.e., a contact area of approximately 1000−5000 nm^2 may be assumed). The number of grafted molecules within that range should in the ideal case be equal to the number of adherent chains as observed in the experiments. That is, by measuring the average number of grafted chains adhering to the tip, the grafting density of polymer chains at the surface may be estimated. For example, when assuming a curvature radius of the silicon nitride probe of 20 nm, a grafting density of $\sigma = 0.002$ chain nm^{-2} is calculated (cf. Discussion of Figure 4 above: an average of three chains is observed within the contact region; thus, $\sigma = 3$ chains/(π(20 nm)^2).

For comparison, the grafting density was also estimated from the signal intensities of carbon and silicon peaks in the XPS spectra. The obtained value of $\sigma = 0.005$ chain nm^{-2} is of the same order of magnitude as the value obtained by AFM. Taking into account the average contour length of the chains estimated both from GPC data and from the plateau length distribution, we can conclude that the average area per grafted chain is comparable to, or larger than, the square gyration radius of the polymer coil. Hence, intermolecular interactions between neighboring grafted chains are weak, at least in the neutral or weakly acidic pH range. (Note that in 100 mM sodium chloride solution the Debye screening length is ∼1 nm so that long-range Coulomb intermolecular interactions are screened off.)

Discussion

The interpretation of the force−extension spectra may be based on a set of established theoretical models. The pulling-off of a neutral polymer chain from an adsorbing substrate in good or theta-solvent was theoretically analyzed in refs 39 and 40. It was demonstrated that the progressive detachment of a preadsorbed chain from the adsorbing surface occurs when a constant pulling force, f_c, is applied to one end of the chain. The magnitude of this pulling force, f_c, which is necessary to induce desorption of the chain, is proportional to the "binding energy" (per monomer) divided by the monomer size. This force, which is directly measured in the AFM experiment, increases with increasing adsorption strength.

Upon the desorption process, the polymer chain can be envisioned as partially desorbed, i.e., consisting of an adsorbed segment (comprising N_{ads} monomers) and a uniformly extended segment (comprising N_{bridge} monomers), bridging the chain end to the adsorbing surface.

The elastic tension in the bridging segment is equal to the desorption force, f_c. Therefore, the degree of extension of the bridging segment, $z/(aN_{bridge}) \sim f_c a/k_B T$, increases with increasing strength of adsorption (here, z is the distance between the tip and the substrate, i.e., the apparent length of the extended bridging segment of the chain, to which the force f_c is applied; a is the monomer length under "zero force"). At strong adsorption, $f_c a/k_B T > 1$, the bridging segment is almost completely extended, that is, $z/(aN_{bridge}) \approx 1$.

The net free energy of the entire polymer chain comprises the (negative) contribution of the adsorbed segment and the entropic penalty for the extension of the bridging segment. If the retreat of the chain end from the surface occurs at an infinitely slow rate, the system can be considered in perfect equilibrium. As the successive detachment of monomers of the adsorbed segment from the tip surface continues, the number of monomers in the extended bridging segment, N_{bridge}, increases, while the number of monomers in the adsorbed chain segment, N_{ads}, decreases. Hereby, the total free energy of the polymer chain continuously increases, as the increasing fraction of monomers in the bridging segment contributes an increasing conformational entropic penalty, while the free energy gain of the adsorbed segment continuously decreases in proportion to the continuously decreasing number of adsorbed monomers. In perfect equilibrium, the resulting net increase of the desorbing polymer chain upon increasing the tip−surface separation by Δz is equal to the stretching energy, $f_c \Delta z$.

At a certain tip−surface distance (i.e., certain length of the extended polymer segment), the free energy gain in the adsorbed segment is exactly counterbalanced by the conformational entropy penalty in the bridge; this distance may be termed z_b. At this point, the adsorbed state of the polymer chain is no longer energetically favored over the desorbed state of the polymer chain, which would thermodynamically favor the full desorption of the remaining adsorbed chain segment at z_b.

However, for complete desorption, the adsorbed segment has to overcome a potential barrier (activation barrier), the height of which is proportional to $(f_c a)^2 N_{ads}/k_B T$ and thus much larger than $k_B T$. This activation barrier provides a kinetic hindrance for the full desorption of the remaining adsorbed chain segments. In perfect equilibrium (i.e., under conditions of infinitely slow stretching), the activation barrier would be overcome by the adsorbed chain segments at a natural off-rate, and full desorption of the entire polymer chain from the tip would be observed at z_b. z_b thus reflects the lowest limit of the experimentally measured "apparent" polymer chain length.

In a real experiment, the stretching rate is finite. Thus, for a sufficiently high activation barrier, the continuous desorption of successive monomers from the tip may continue even upon an increase in $z > z_b$. Hereby, the necessary pulling force, f_c, remains constant, and the system follows a sequence of metastable states with decreasing number of monomers N_{ads} in the adsorbed segment. Hereby, the (unfavorable) elastic free energy in the bridge continues to rise as N_{bridge} increases and the (favorable) adsorption energy of the adsorbed segment continues to fall as N_{ads} decreases. Simultaneously, as N_{ads} decreases, the height of the free energy barrier decreases as well and will become of the order of $k_B T$ at a point, which may be termed $z = z_s > z_b$. That is, the barrier separating the adsorbed state of the polymer chain from the desorbed state of the polymer chain becomes of the order of $k_B T$. z_s therefore reflects the maximum "apparent" chain length, which may be observed under the real experimental conditions of finite stretching rates, which will not always be reached as stochastic fluctuations may naturally drive the system also over activation barriers larger than $k_B T$.

However, the larger the adsorption strength of the adsorbed monomers at the tip surface is, the larger will be, both, the free energy contribution of the adsorbed monomers and the potential barrier between the adsorbed and the desorbed state of the polymer chain (i.e., the activation barrier for full desorption). As a result, z_s will become larger, too. Namely, the experimen-

tally observed z_s will become comparable to the actual polymer chain length, L.

It should be noted that, in contrast to the unbinding of single molecular bonds, such as ligand−receptor bonds, which have been extensively studied by force spectroscopy,[9,41,42] in the continuous desorption process of polymer chains two different types of unbinding events need to be considered: the successive unbinding of individual segments (which repeatedly occurs in a zipper-type mechanism) and the instantaneous and complete desorption of the adsorbed polymer chain end (in which, ultimately, all remaining adsorbed segments detach at once). The unbinding of an individual segment occurs at a much higher speed than the pulling rates accessible in the AFM experiment. Thus, no dependence of the plateau force, which resembles the unbinding force of individual segments, is observed. However, there is a rate dependence of the observed unbinding length originating from the second "unbinding event". As discussed above, during the desorption process, the remaining adsorbed chain end continuously shortens. As a result, the "bond" between the adsorbed polymer chain end and the substrate becomes continuously weaker until, at a critical length, its unbinding rate becomes comparable to the experimental pulling speed. Upon varying the pulling speed, this critical length of the remaining adsorbed polymer end naturally varies as well. Thus, the observed critical length is a function of pulling speed, and thus is the "apparent" chain length, while the unbinding force is *not* rate-dependent (as it is always limited by the unbinding force of the ongoing process of the continuous desorption of the individual segments). Note that if the adsorption strength is high, the critical point is reached very close to the actual chain end.

While our model neglects excluded-volume interactions and/or finite extensibility of the chain, the following main trends remain valid: (i) the detachment distance z_s is proportional to the contour length L of the chain, $z_s = \varphi L$, and (ii) the proportionality coefficient φ increases with increasing adsorption strength, approaching unity for strong adsorption.

Hence, the distribution of the detachment lengths, z_s, measured in the AFM experiment can be directly related (with a rescaling factor that depends on the adsorption strength) to the molecular weight distribution in the ensemble of the polymer chains probed in the pulling-off experiment. For strong adsorption, the distribution of desorption lengths measured by AFM should directly resemble the distribution of the polymers' contour lengths (i.e., their "real" molecular weight distribution).

The adsorption of poly(acrylic acid) chains onto the negatively (that is, similarly) charged silicon nitride (effectively, silicon oxide) surface of the tip is nonelectrostatically driven. Moreover, the fraction of charged monomers (equal to the degree of ionization) and the surface charge density are simultaneously affected in the present system by the variation of the pH. For a PAA chain interacting with the tip surface, both, the repulsive intramolecular Coulomb interaction and the polymer−surface interaction are pH-dependent via the pH-dependent degrees of ionization of AA monomers and Si−OH functions on the tip surface. The observed pH dependence of the measured plateau lengths may therefore be interpreted in terms of decreasing strength of adsorption at high pH, resembling a decrease in the force-dependent proportionality factor φ. Indeed, upon an increase in pH, the negative ionic charge of both the adsorbed segments of the PAA chains and the tip surface are known to increase. Therefore, the Coulomb repulsion between the polymer and the surface becomes stronger and the adsorption strength between the tip surface and the PAA chains becomes weaker, which is also reflected in the decrease of the measured desorption forces at high pH.

PAA is a weak acid; the pK_a for individual AA monomer is ∼5.5. In the polymer, the dissociation of AA units results in an intramolecular Coulomb repulsion between dissociated, and thus negatively charged, neighboring carboxylic groups. Therefore, the effective pK of AA units in a polymer is larger and depends on the salt concentration (the pK decreases with increasing ionic strength of the solution due to screening of intramolecular Coulomb interaction). Moreover, segments of PAA chains adsorbed onto the negatively charged surface are ionized less than those far from the surface due to the lower local electrostatic potential (lower local pH) in the vicinity of the negatively charged surface.[38]

At pH > pK, most of the monomers are ionized, and intramolecular Coulomb repulsion (partially screened by salt) acts as an excluded-volume interaction ensuring the swelling of the grafted polymer chains. This scenario therefore holds true for the above discussion of our results in neutral to alkaline aqueous buffer, which thus constitutes a good solvent for PAA.

Below approximately pH 5.5, when the carboxylate groups become protonated and thus uncharged, the quality of water as a solvent for PAA significantly decreases. The variation of pH in our experiments therefore has a similar effect as the variation of the solvent strength in the case of nonionic polymers.

The high polymer density in the collapsed PAA chain suppresses the ionization of monomers due to the lowering of the local electrostatic potential and the decreasing of the effective dielectric constant of the medium. As a result, the collapse transition within individual chains occurs discontinuously, so that collapsed (weakly ionized) and swollen (ionized) states may coexist.[43]

If a collapsed polymer globule (with dominating attractive monomer−monomer interactions under poor solvent conditions) is brought into contact with the adsorbing tip surface, the following scenarios can be distinguished:[44] (i) Monomer−monomer attraction is stronger than the monomer−surface attraction. Then, no significant perturbation in the globule conformation (no adsorption to the tip) takes place. (ii) Monomer−surface attraction is stronger than monomer−monomer attraction. Then, the globule spreads on the surface (strong adsorption) and the detachment of the adsorbed chain by the applied pulling-off force occurs similarly to the scenario described above. (iii) Monomer−monomer and monomer−surface attraction are comparable, and the globule adsorbs onto the surface ("wets" the surface with a finite contact angle). In this "transition regime" more sophisticated patterns in the detachment force−extension spectra are to be expected. The distribution of the plateau lengths can no longer be directly recalculated into a molecular length distribution.

In the pH range around pH 5, the PAA chains in the solution (and the bridging segments) are slightly protonated (marginally good solvent quality of water), while the surface charge density is still large (pK of the surface OH groups is around 2−3). As a result, the local pH in the vicinity of the surface may drop below the pK of PAA. This may cause the collapse of the chain segments proximal to the surface.

A second important effect in this pH regime is the possible adsorption of the grafted polymer chains on the substrate. In this context, it is important to note that the silica substrate is modified by silanization prior to polymerization, which means that it has a different, i.e., more hydrophobic, character than the bare silica tip. It is therefore reasonable to assume that adsorption of the (slightly protonated) grafted poly(acrylic acid) chains becomes more favorable and thus competes with tip

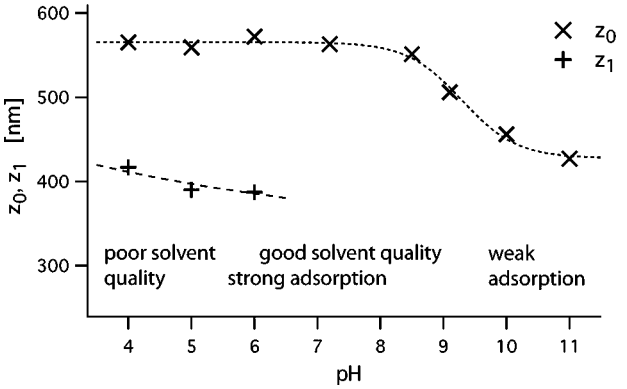

Figure 8. Measured maxima of the length distributions in dependence of the pH of the aqueous buffer (see also Figure 5).

adsorption. As has been demonstrated earlier,[45] an enhanced attraction to the grafting surface generally leads to a segregation of grafted chains into two populations: adsorbed and extended ones. These different chain conformations may result in the appearance of the bimodal plateau length distribution. Further analysis, including the study of grafted polymer layers with higher grafting density, will help to elucidate this effect.

When the pH is further lowered (pH 4−pH 2), the acrylic acid groups become fully protonated. In addition, the SiOH groups on the tip surface also get protonated; i.e., both the intramolecular and polymer−surface Coulomb repulsion vanish. The distribution of the measured plateau lengths flattens off, while the average length decreases as compared to that measured at high pH. This reflects a variety of different metastable states upon pulling-off the collapsed PAA chain from the tip surface. Hence, in this pH range, there is no simple relation between observed distribution of the plateau length and molecular weight distribution of grafted polymers.

Note that, generally, a quantitative prediction of the desorption force magnitude is not possible since the relevant adsorption energy comprises several contributions, which cannot be calculated unambiguously. For example, the magnitude of short-range van der Waals attractions depends strongly on the polymer−substrate distance (which cannot be predicted), while the Coulomb repulsion depends on the unknown surface charge density or surface potential. Nevertheless, our results qualitatively support our theoretical model, as we have demonstrated that an increase in pH, which is expected to lower the net adsorption strength, indeed results in decreasing plateau length and force magnitude.

Figure 8 shows a summary of our observations. It illustrates the effects of poor solvent quality (splitting of the desorption length distribution at low pH) as well as the effects of weak polymer−tip adsorption (decrease of the average desorption length at high pH). In the intermediate regime, the desorption length distribution measured by AFM reflects the molecular length distribution of PAA as determined by GPC. On the basis of our discussion above, it is thus concluded that AFM desorption measurements allow for the analysis of the molecular length distribution of substrate-grafted polymers in the regime of good solvent quality and strong tip adsorption.

Summary

We have applied AFM-based force spectroscopy for the characterization of monolayers of end-grafted poly(acrylic acid) (PAA) chains, which were obtained by means of surface-initiated nitroxide-mediated polymerization from a silica surface. The distribution of the characteristic desorption lengths of the polymer chains in the measured force−extension curves and their corresponding desorption forces were recorded under conditions of varying pH of the aqueous buffer solution. Hereby, the plateau length distributions were found to depend not only on the real chain length of the grafted polymers but also on the chain conformation governed by intramolecular interactions and solvent quality as well as the strength of adsorption of AA monomers on the AFM tip. This relationship follows from known theories, and it is confirmed by comparison to the GPC data on free polymers. For sufficiently good solvent quality and strong adsorption of the polymer chains to the AFM tip, the desorption length distribution coincides with the molecular length distribution of the substrate-grafted polymers. The latter can thus be directly measured in AFM desorption experiments.

Acknowledgment. The work was financially supported by Deutsche Forschungsgemeinschaft (DFG) through SFB 486 and by Deutscher Akademischer Austauschdienst (DAAD) and EGIDE through the PROCOPE program. J.P. gratefully acknowledges financial support by Marie Curie Fellowship.

References and Notes

(1) Fischer, H. *J. Am. Chem. Soc.* **1986**, *108*, 3925−3927.
(2) Fischer, H. *Macromolecules* **1997**, *30*, 5666−5672.
(3) von Werne, T.; Patten, T. E. *J. Am. Chem. Soc.* **2001**, *123*, 7497−7505.
(4) Matyjaszewski, K. *J. Phys. Org. Chem.* **1995**, *8*, 197−207.
(5) Matyjaszewski, K. *Macromol. Symp.* **2001**, *174*, 51−67.
(6) Matyjaszewski, K. *Curr. Opin. Solid State Mater. Sci.* **1996**, *1*, 769−776.
(7) Matyjaszewski, K.; Miller, P. J.; Shukla, N.; Immaraporn, B.; Gelman, A.; Luokala, B. B.; Siclovan, T. M.; Kickelbick, G.; Vallant, T.; Hofmann, H.; Pakula, T. *Macromolecules* **1999**, *32*, 8716−8724.
(8) Georges, M. K.; Veregin, R. P. N.; Kazmair, P. M.; Hamer, G. K. *Macromolecules* **1993**, *26*, 2987−2988.
(9) Florin, E. L.; Moy, V. T.; Gaub, H. E. *Science* **1994**, *264*, 415−417.
(10) Rief, M.; Oesterhelt, F.; Heymann, B.; Gaub, H. E. *Science* **1997**, *275*, 1295−1297.
(11) Clausen-Schaumann, H.; Seitz, M.; Krautbauer, R.; Gaub, H. E. *Curr. Opin. Chem. Biol.* **2000**, *4*, 524−530.
(12) Janshoff, A.; Neitzert, M.; Oberdörfer, Y.; Fuchs, H. *Angew. Chem., Int. Ed.* **2000**, *39*, 3213−3237.
(13) Goodman, D.; Kizhakkedathu, J. N.; Brooks, D. E. *Langmuir* **2004**, *20*, 6238−6245.
(14) Grandbois, M.; Beyer, M.; Rief, M.; Clausen-Schaumann, H.; Gaub, H. E. *Science* **1999**, *283*, 1727−1730.
(15) Rief, M.; Gautel, M.; Oesterhelt, F.; Fernandez, J. M.; Gaub, H. E. *Science* **1997**, *276*, 1109−1112.
(16) Minko, S.; Roiter, Y. *Curr. Opin. Colloid Interface Sci.* **2005**, *10*, 9−15.
(17) Hugel, T.; Grosholz, M.; Clausen-Schaumann, H.; Pfau, A.; Gaub, H. E.; Seitz, M. *Macromolecules* **2001**, *34*, 1039−1047.
(18) Senden, T. J.; di Meglio, J.-M.; Auroy, P. *Eur. Phys. J. B* **1998**, *3*, 211−216.
(19) Chatellier, X.; Senden, T. J.; Joanny, J.-F.; Meglio, J.-M. d. *Europhys. Lett.* **1998**, *41*, 303−308.
(20) Conti, M.; Bustanji, Y.; Falini, G.; Ferruti, P.; Stefoni, S.; Samori, B. *ChemPhysChem* **2001**, *2*, 610−613.
(21) Seitz, M.; Friedsam, C.; Jöstl, W.; Hugel, T.; Gaub, H. E. *ChemPhysChem* **2003**, *4*, 986−990.
(22) Friedsam, C.; Becares, A. D. C.; Jonas, U.; Seitz, M.; Gaub, H. E. *New J. Phys.* **2004**, *6*, Art. No. 9.
(23) Li, H.; Liu, B.; Zhang, X.; Gao, C.; Shen, J.; Zou, G. *Langmuir* **1999**, *15*, 2120−2124.
(24) Al-Maawali, S.; Bemis, J. E.; Akhremitchev, B. B.; Leecharoen, R.; Janesko, B. G.; Walker, G. C. *J. Phys. Chem. B* **2001**, *105*, 3965−3971.
(25) Parvole, J.; Billon, L.; Montfort, J. P. *Polym. Int.* **2002**, *51*, 1111−1116.
(26) Parvole, J.; Laruelle, G.; Guimon, C.; Francois, J.; Billon, L. *Macromol. Rapid Commun.* **2003**, *24*, 1074−1078.
(27) Husemann, M.; Morrison, M.; Benoit, D.; Frommer, J.; Mate, C. M.; Hinsberg, W. D.; Hedrick, J. L.; Hawker, C. J. *J. Am. Chem. Soc.* **2000**, *122*, 1844−1845.
(28) Bartholome, C.; Beyou, E.; Bourgeat-Lami, E.; Chaumont, P.; Zydowicz, N. *Macromolecules* **2003**, *36*, 7946−7952.

(29) Laruelle, G.; Parvole, J.; Francois, J.; Billon, L. *Polymer* **2004**, *45*, 5013−5020.
(30) Parvole, J.; Montfort, J. P.; Billon, L. *Chem. Phys.* **2004**, *205*, 1369−1378.
(31) Prucker, O.; Rühe, J. *Macromolecules* **1998**, *31*, 592−601.
(32) All samples to be compared were prepared on the same silicon wafer.
(33) Laruelle, G.; Francois, J.; Billon, L. *Macromol. Rapid Commun.* **2004**, *25*, 1839−1844.
(34) Couvreur, L.; Lefay, C.; Belleney, J.; Charleux, B.; Guerret, O.; Magnet, S. *Macromolecules* **2003**, *36*, 8260−8267.
(35) Butt, H.-J.; Jaschke, M. *Nanotechnology* **1995**, *6*, 1−7.
(36) Maschio, G.; Scali, C. *Macromol. Chem. Phys.* **1999**, *200*, 1708−1721.
(37) Israels, R.; Leermakers, F. A. M.; Fleer, G. J. *Macromolecules* **1994**, *27*, 3087−3093.
(38) Borisov, O. V.; Boulakh, A. B.; Zhulina, E. B. *Eur. Phys. J. E* **2003**, *12*, 543−551.
(39) Eisenriegler, E.; Kremer, K.; Binder, K. *J. Chem. Phys.* **1982**, *77*, 6296−6320.
(40) Klushin, L. I.; Skvortsov, A. M.; Leermakers, F. A. M. *Phys. Rev. E* **2002**, *66*, 036114.
(41) Evans, E.; Ritchie, K. *Biophys. J.* **1997**, *72*, 1541−1555.
(42) Merkel, R.; Nassoy, P.; Leung, A.; Ritchie, K.; Evans, E. *Nature (London)* **1999**, *397*, 50−53.
(43) Raphael, E.; Joanny, J.-F. *Europhys. Lett.* **1990**, *13*, 623−628.
(44) Johner, A.; Joanny, J.-F. *J. Phys. II* **1991**, *1*, 181−194.
(45) Zhulina, E. B.; Borisov, O. V.; van Male, J.; Leermakers, F. A. M. *Langmuir* **2001**, *17*, 1277−1293.

MA0505880